NATO OTAN NURC
a NATO Research Centre
un Centre de Recherche de l'OTAN
NURC PARTNERING FOR MARITIME INNOVATION

Reprint Series **NURC-PR-2009-001**

3D target shape from SAS images based on a deformable mesh

Enrique Coiras, Johannes Groen

December 2009

Originally published in:

Proceedings of the 3rd International Conference and Exhibition on Underwater Acoustic Measurements: Technologies and Results, 21-26 June, 2009, Nafplion, Greece.

About NURC

Our vision

- To conduct maritime research and develop products in support of NATO's maritime operational and transformational requirements.
- To be the first port of call for NATO's maritime research needs through our own expertise, particularly in the undersea domain, and that of our many partners in research and technology.

One of three research and technology organisations in NATO, NURC conducts maritime research in support of NATO's operational and transformation requirements. Reporting to the Supreme Allied Commander, Transformation and under the guidance of the NATO Conference of National Armaments Directors and the NATO Military Committee, our focus is on the undersea domain and on solutions to maritime security problems.

The Scientific Committee of National Representatives, membership of which is open to all NATO nations, provides scientific guidance to NURC and the Supreme Allied Commander Transformation.

NURC is funded through NATO common funds and respond explicitly to NATO's common requirements. Our plans and operations are extensively and regularly reviewed by outside bodies including peer review of the science and technology, independent national expert oversight, review of proposed deliverables by military user authorities, and independent business process certification.

NOTE: The NURC Reprint series reprints papers and articles published by NURC authors in the open literature as an effort to widely disseminate NURC products. Users should cite the original article where possible.

3D TARGET SHAPE FROM SAS IMAGES BASED ON A DEFORMABLE MESH

Enrique Coiras[a], Johannes Groen[a]

[a]NATO Undersea Research Centre. Viale San Bartolomeo 400. 19126 La Spezia. Italy.

Contact author: Enrique Coiras, Email: coiras@nurc.nato.int, Fax: +39-0187527330.

Abstract: *The seafloor can nowadays be scanned with side-looking sonar that provides a very high resolution over a large swath, which has proved beneficial for underwater target detection and classification. For systems operated at hundreds of kilohertz, one may obtain centimeter resolution in the range and along-track direction. For these systems, the third dimension, height, is usually resolved much worse. Since the 3D shape is regarded a valuable clue in underwater target classification, it is important to extract height information as best as possible. In this paper a new method for deriving 3D information from non-interferometric SAS images is described. The method is experimentally applied to multi-view reconstruction of calibrated target shapes imaged by the MUSCLE vehicle, and the results are compared to the actual dimensions of the observed objects in order to quantify the reconstruction accuracy. The reconstruction algorithm is a shape-from-shading approach that uses a deformable mesh to preserve surface continuity while enforcing observational constraints. The technique is shown to have an important impact in object classification, both as a stand-alone method and combined with other 3D imaging techniques such as interferometry. Implications to target identification and vehicle autonomy are discussed.*

Keywords: *Synthetic Aperture Sonar, 3D reconstruction, Shape from Shading.*

1. INTRODUCTION

Modern side-looking sonars provide a very high resolution over a large swath, which has proved beneficial for underwater target detection and classification. For systems operated at hundreds of kilohertz, one may obtain centimetre resolution in range and along-track directions. The third dimension, height, is usually resolved much worse, and as a consequence indirect methods—such as measuring shadow length—are frequently used to estimate the height of objects. Nevertheless, since not just the height but in fact the complete 3D shape of an object is an invaluable clue for underwater target classification, it is important to extract as much detailed height information as possible from the existing sonar image data. In this paper we present a new method for deriving 3D information from non-interferometric SAS images that uses a deformable mesh to solve the constraint satisfaction problem posed by a basic shape-from-shading approach.

2. 3D RECONSTRUCTION BASED ON A DEFORMABLE MESH

The underlying idea behind shape-from-shading [1] is that the configuration of a surface can be inferred from observing the way it reflects and scatters light (or sound in the case of sonar). And, in effect, the intensity of the reflected signal when illuminated by a sonar sensor is mostly dependent on surface slopes: the more directly the local normal vector of the surface faces the sonar, the brighter the image pixel for that location will be.

The simplest model for this type of behaviour is Lambert's law [2], which assumes diffuse scattering and results in the returned intensity I from surface point $\mathbf{p}$ being proportional to the cosine of the angle θ formed by the direction of observation $\mathbf{r}$ and the surface's normal vector $\mathbf{N}$:

$$I\big(x(\mathbf{p}), y(\mathbf{p})\big) \propto \mathbf{r}(\mathbf{p}) \cdot \mathbf{N}(\mathbf{p}) = \cos\theta(\mathbf{p}) \tag{1}$$

Where x and y are the coordinates of the pixel where surface point p appears in image I.

More complex models [3] can take into account the type of material forming the surface (its composition, granularity, etc). The inclusion of specular effects is another possibility, and is often implemented as a power function of the basic cosine law.

2.1. Local formulation in polar coordinates

Equation (1) provides a link between the observed intensities in a sonar image and the local orientation of the observed surfaces. To exploit this link in order to derive surface topography, working in polar coordinates has several advantages. The main one is the slopes being constant and independent of local elevation, which speeds up the iterative optimization algorithm. The derivation of the formulas is a bit more involved than when working on Cartesian coordinates (as in [2]), but the consequent simplification of the iterative optimization process more than compensates for it, especially given the associated speed increase and the ease of adapting the algorithm to a GPU implementation [4].

Sonar images are "range images", with the across-track coordinate x corresponding to the distance r from the surface point to the sonar. This corresponds to a cylindrical coordinate

system centered at the sensor's position **o** and with the cylindrical axis *y* aligned with the direction of travel of the sonar. Two pixels adjacent in the range direction (Fig. 1) have ranges r_i and $r_{i+1}=r_i+dr$, with *dr* being the range resolution (which in the case of SAS is constant).

Thus, for every range image pixel two of the three cylindrical coordinates are known (*y* and *r*), whereas the angular coordinate α (depression or grazing angle from the sensor) is not. An estimation of this coordinate's derivative for a given pixel can nevertheless be obtained from the image intensity at the pixel [2].

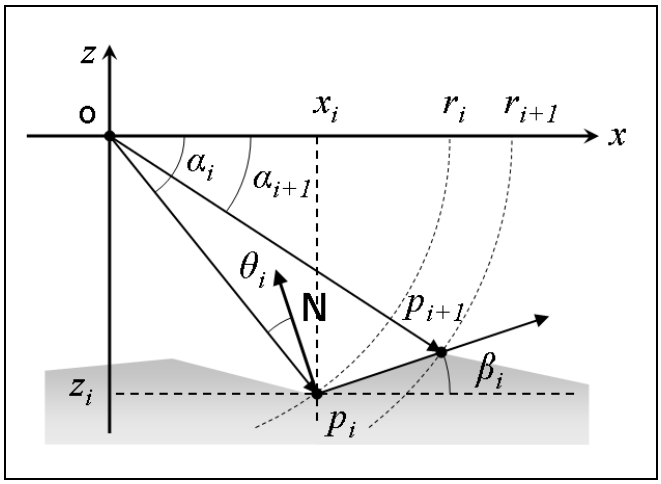

Fig.1: Polar formulation of the geometry for the 3D reconstruction problem of a single scan line.

In effect, with our choice of coordinates and assuming Lambert's imaging model, the intensity at a point p_i directly depends on the angle θ_i formed by a radius **r** and the surface normal **N** at the point. The surface tangent at a point p_i is a 3D vector (*dr*, *dy*, *dα*) with *dr* the sonar's range resolution and where we initially assume *dy* is zero. The value of *dα* is given by the intersection of a secant line at p_i (tilted by θ_i from the tangent's direction) with the circle of radius $r_{i+1}=r_i+dr$.

Computation of *dα* is straightforward after noting that it does not depend on α_i. By a change of coordinates ($\alpha=\alpha-\alpha_i$, thus setting α_i to zero) we can use the simplified diagram on Fig.2 to derive the expression for *dα*.

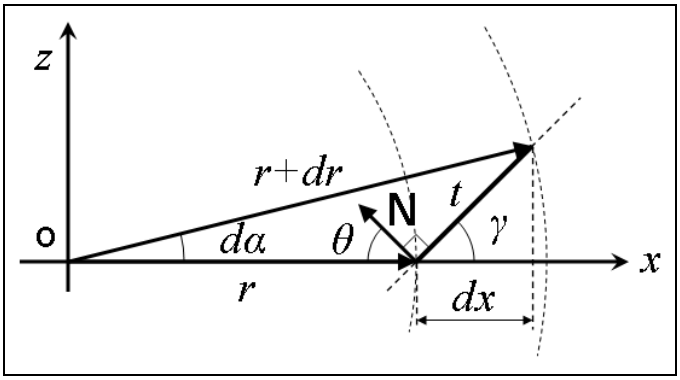

Fig.2: A change of coordinates simplifies the derivation of an expression for dα.

Applying the cosine theorem to the triangle formed by *r*, *r+dr* and *t*, we obtain:

$$t^2 = r^2 + (r + dr)^2 - 2r(r + dr)\cos(d\alpha) \tag{2}$$

Additionally, it is clear from Fig.2 that:

$$dx = (r + dr)\cos(d\alpha) - r \tag{3}$$

$$dx = t\cos(\gamma) = t\cos\left(\frac{\pi}{2} - \theta\right) = t\sin(\theta) \tag{4}$$

Combination of (2), (3) and (4) yields the final expression for the $d\alpha$:

$$\cos(d\alpha) = \frac{1}{r + dr}\left(-r\sin^2\theta + r + \sqrt{r^2\sin^4\theta + dr^2\sin^2\theta + 2rdr\sin^2\theta}\right) \tag{5}$$

The $d\alpha_{ij}$ for every image pixel (i, j) can thus be obtained substituting in (5) the value of θ that corresponds to intensity $I(i, j)$ according to the selected illumination model.

2.2. Derivation of the global solution

Knowing the altitude of the sonar over the seafloor (from the first-returns in the range image or from navigation data), the absolute values of α for the image pixels at minimum range r_0 can be set, therefore allowing for the derivation of the α coordinate of any pixel by simple integration:

$$\alpha_{ij} = \alpha(r_{ij}) = \alpha_{oj} + \int_{r_{oj}}^{r_{ij}} d\alpha_{ij}(r) \approx \alpha_{oj} + \sum_{k=0}^{i} d\alpha_{kj} \tag{6}$$

Unfortunately the $d\alpha$ obtained from Lambert's diffuse model are just an approximation and the 3D reconstruction resulting by just applying (6) to each image line is extremely noisy. And since the method works line-by-line the reconstructed surface gets jaggier as range increases. Results can be smoothed out by directly enforcing surface continuity ($\alpha_{ij} - \alpha_{ij+1} \approx 0$), ensuring that adjacent lines don't diverge too much from each other—although this has the undesirable effect of also smoothing the details of the reconstructed surfaces.

In order to minimize the unwanted smoothing effects of enforcing continuity, we have weighted it using two simple heuristics that have provided good results:

- Adjacent pixels of similar intensity are likely to belong to the same surface patch. This follows from the natural assumption that edges in the image likely correspond to boundaries between objects in the scene.
- Dark pixels provide less information than bright ones, and in fact nothing is known about completely shadowed pixels.

The two rules can be incorporated in a weighted expression that determines the along-track relation between adjacent pixels:

$$\alpha_{ij} = \frac{\left(I_{ij-1}\left(1-\left|I_{ij}-I_{ij-1}\right|\right)\right)^f \alpha_{ij-1} + \left(I_{ij+1}\left(1-\left|I_{ij}-I_{ij+1}\right|\right)\right)^f \alpha_{ij+1}}{\left(I_{ij-1}\left(1-\left|I_{ij}-I_{ij-1}\right|\right)\right)^f + \left(I_{ij+1}\left(1-\left|I_{ij}-I_{ij+1}\right|\right)\right)^f} \tag{7}$$

Where I_{ij} has been used instead of $I(i, j)$ for conciseness and where f is a power factor between 0 and 1. Note that here we assume the image I has been already normalized to the [0, 1] range with 0 corresponding to the shadows (-5dB) and 1 to the highlights (35dB).

With the constraints given by equations (6) and (7) any α_{ij} can be related to its neighbors and a global solution can be found by solving a system of linear equations. Unfortunately the system is very sparse and nearly singular, which makes solving it problematic. A regularization scheme is required, which results in over-smoothed solutions and long computation times.

An alternative approach to finding the global solution is to formulate the reconstructed surface as a deformable elastic mesh (Fig. 3) and pose the constraints as forces that deform it. The mesh can be left to evolve over time until it converges to an equilibrium configuration, which will correspond to the sought reconstruction surface. Note that for simplicity Fig.3 shows a Cartesian mesh, where surface points p_{ij} are only allowed to move in the z direction in order to satisfy the constraints to their neighbors. In our cylindrical coordinates implementation the surface points actually displace in the angular coordinate α.

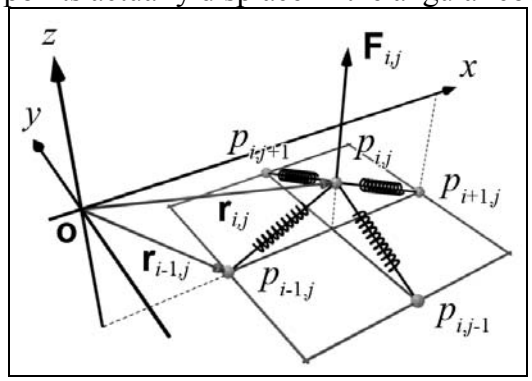

Fig.3: The constraint satisfaction problem posed as a deformable mesh, with the constraints implemented as forces acting on the mesh nodes.

The resultant force $F_{i,j}$ acting on each mesh node consists of two across-track forces ($C_{i,j}^-$ and $C_{i,j}^+$) and two along-track ones ($L_{i,j}^-$ and $L_{i,j}^+$):

$$F_{ij} = C_{ij}^- + C_{ij}^+ + k_L\left(L_{ij}^- + L_{ij}^+\right) \tag{8}$$

Where k_L is a constant that gives more or less weight to the smoothing associated to enforcing continuity (we normally set it to 1/32) and where the forces are:

$$C_{ij}^- = \left(\alpha_{i-1\,j} - \alpha_{ij}\right) + d\alpha_{i-1\,j};\; C_{ij}^+ = \left(\alpha_{i+1\,j} - \alpha_{ij}\right) - d\alpha_{ij} \tag{9}$$

$$L_{ij}^- = \left(I_{ij}I_{ij-1}\left(1-\left|I_{ij}-I_{ij-1}\right|\right)\right)^f \left(\alpha_{ij-1} - \alpha_{ij}\right);\; L_{ij}^+ = \left(I_{ij}I_{ij+1}\left(1-\left|I_{ij}-I_{ij+1}\right|\right)\right)^f \left(\alpha_{ij+1} - \alpha_{ij}\right) \tag{10}$$

Since we are not really interested in the dynamic behavior of the mesh, once the forces are computed at each iteration of the optimization loop, the positions of the mesh nodes are updated by first order evolution:

$$\alpha_{ij} = \alpha_{ij} + k_F F_{ij} \tag{11}$$

Where k_F is a constant that controls the evolution speed (normally set to 0.3). The system is left to evolve until the forces are small enough that an equilibrium configuration can be assumed. The whole algorithm is implemented in a multi-resolution fashion similar to that of [2].

3. RESULTS

The proposed reconstruction method has been applied to SAS images acquired with NURC's MUSCLE vehicle. One example is shown in Fig.4, where the 3D has been estimated for a set of jars found in the wreck of the roman vessel Dolia.

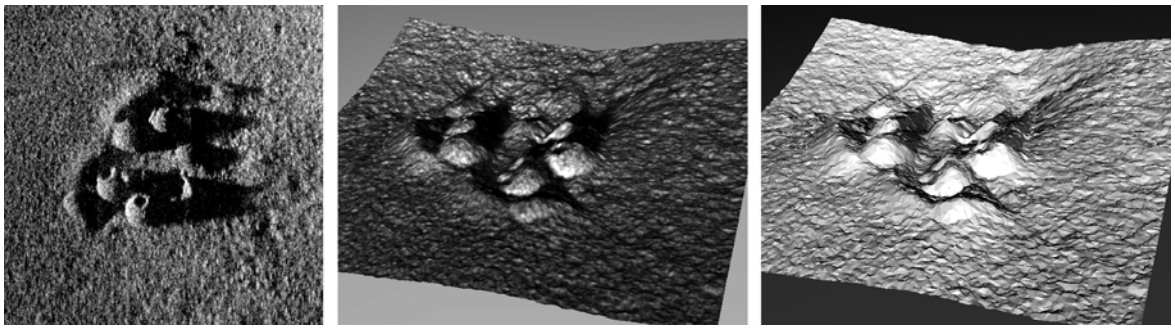

Fig.4: Single-view reconstruction results for a set of roman jars found in the Dolia wreck. Left: MUSCLE SAS image. Middle: textured 3D surface. Right: flat shaded 3D.

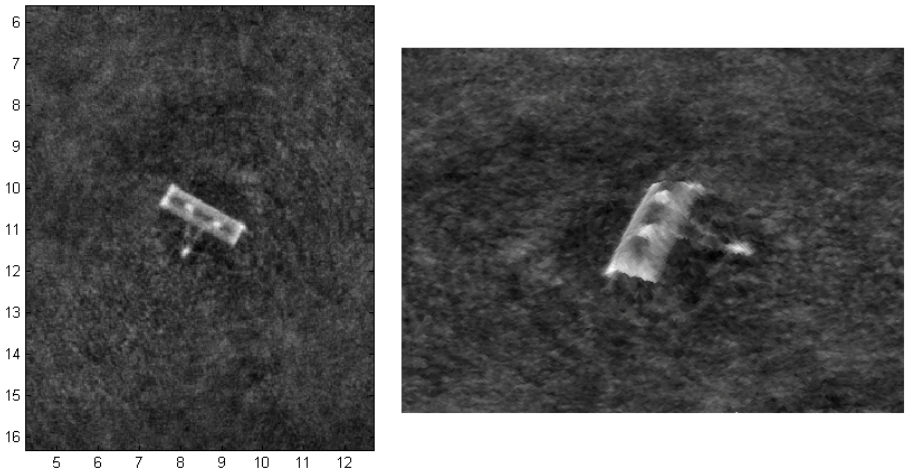

Fig.5: Multi-view reconstruction results for a 2m cylindrical target. Left: combination of the 15 different views after registration of the 3D reconstructions. Right: textured 3D.

Application of the method to multi-view reconstruction of underwater targets provides unprecedented shape details that should improve classification and identification performance [5]. Fig. 5 shows the results for the combination of 15 views of a cylindrical exercise target during the Colossus2 trials in Latvia (2008).

Combination of the 3D surfaces obtained from different views is nevertheless not trivial: navigation accuracy is not enough to just merge the geo-referenced reconstructions, areas within the shadow volumes must be discarded, and the reconstructions are only resolved up to a single-valued elevation map that is distorted by the shape of its imaging wave-front [6]. The result shown in Fig. 5 has been obtained by correlation of the different surfaces with the

shadow areas masked out and weighting elevation values according to their echo strengths, but the method still needs further development for improved robustness and accuracy.

4. DISCUSSION

The proposed technique should have an important impact in object classification, given the amount of detail that it can provide (in principle up to sensor's pixel resolution). Combination with interferometry should also give more accurate reconstructions.

We are now working on a GPU implementation of the iterative optimization algorithm which we expect should provide a speed increase of several orders of magnitude [4]. This should open the possibility for novel detection and classification applications that were until now unfeasible due to their prohibitive computational costs.

5. ACKNOWLEDGEMENTS

The authors would like to thank Dr. Mario Zampolli, scientist in charge of the Dolia campaign (Italy), and Dr. Benjamin Evans, scientist in charge of the Colossus2 trial (Latvia).

REFERENCES

[1] **R. Z hang, P. Tsai, J. Cryer, and M. Shah** , "Shape from shading: a survey," *IEEE Trans. Pattern Anal. Mach. Intell.*, vol. 21, no. 8, pp.690–706, Aug. 1999.

[2] **E. Coiras, J. Groen**, "Simulation and 3D Reconstruction of Side-looking Sonar Images", book chapter in "Advances in Sonar Technology", In-Tech Books, Vienna, Austria, pp.1-14, 2009. http://intechweb.org/book.php?id=142

[3] **S. Stanic, K. B. Briggs, P. Fl eischer, R. I. Ray, W. B. Saw yer**, "Shallow water high frequency bottom scattering off Panama City, Florida," *J. Acoust. Soc. Amer.*, vol. 83, no. 6, pp. 2134–2144, 1988.

[4] **E. Coiras, A. Ramirez-Montesinos, J. Groen** , "GPU-based Simulation of Side-looking Sonar Images", In *Proceedings of the Oceans'09 IEEE Bremen conference*, Bremen, Germany, 2009.

[5] **E. Coiras, J. Groen, V. Myers, B. Evans** , "Estimation of 3D Shape from High-Resolution Sonar Imagery for Target Identification", In *Proceedings of the IoA DCUT 2007 conference*, Edinburgh, UK, 2007.

[6] **E. Coiras, Y. Petillo t, D. M. Lane** , "Multi-Resolution 3D Reconstruction from Side-Scan Sonar Images", In *IEEE Transactions on Image Processing*, Vol. 16, No. 2, pp. 382-390, February 2007.

Document Data Sheet

Security Classification		Project No.
Document Serial No.	**Date of Issue**	**Total Pages**
NURC-PR-2009-001	December 2009	7 pp.

Author(s)

Coiras, E., Groen, J.

Title

3D target shape from SAS images based on a deformable mesh.

Abstract

Keywords

Issuing Organization

NURC
Viale San Bartolomeo 400, 19126 La Spezia, Italy

[From N. America:
NURC
(New York) APO AE 09613-5000]

Tel: +39 0187 527 361
Fax:+39 0187 527 700

E-mail: library@nurc.nato.int